

AD-A101 311 YALE UNIV NEW HAVEN CT DEPT OF ENGINEERING AND APPL--ETC F 6 7/4  
CALCULATIONS ON DISSOCIATIVE ATTACHMENT TO HCl. HCl+E YIELDS H+-ETC(IU)  
JUN 81 A HERZENBERG  
N00014-80-K-0595  
NL

UNCLASSIFIED

1

100 1  
200 200

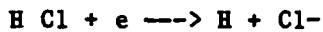
END  
DATE  
FILED  
8-8-81  
DTIC

AD A101311

LEVEL

7

CALCULATIONS ON DISSOCIATIVE ATTACHMENT TO HCl:



ONR contract N00014-80-K-0595

A. Herzenberg

Dept. of Engineering and Applied Science,  
Yale University,  
P.O. Box 2157, Yale Station, New Haven, Conn. 06520

S 14 JUL 1981  
H

This document has been approved  
for public release and sale; its  
distribution is unlimited.

81 7 13 077

FILE COPY

## SECURITY CLASSIFICATION OF THIS PAGE (When Data Entered)

REPORT DOCUMENTATION PAGE		READ INSTRUCTIONS BEFORE COMPLETING FORM
1. REPORT NUMBER <i>(14) 1</i>	2. GOVT ACCESSION NO. <i>AD-4707322</i>	3. RECIPIENT'S CATALOG NUMBER
4. TITLE (and Subtitle) <i>CALCULATIONS ON DISSOCIATIVE ATTACHMENT TO HCl</i>	5. TYPE OF REPORT & PERIOD COVERED Final Report March 1980 - 10.31.1980	
6. AUTHOR(s) <i>Arvid Herzenberg</i>	7. PERFORMING ORG. REPORT NUMBER <i>N00014-80-K-0595</i>	
8. PERFORMING ORGANIZATION NAME AND ADDRESS Dept. of Engineering and Applied Science Yale University, P.O. Box 2157 Yale Station New Haven, Connecticut 06520	10. PROGRAM ELEMENT, PROJECT, TASK AREA & WORK UNIT NUMBERS NR 393-048/1-25-80 (421) <i>11 30 Jun 84</i>	
11. CONTROLLING OFFICE NAME AND ADDRESS Office of Naval Research, Resident Representative 715 Broadway 5th Floor New York, New York 10003	12. REPORT DATE June 30, 1981	
14. MONITORING AGENCY NAME & ADDRESS (if different from Controlling Office) Director, Physics Program Physical Sciences Division Office of Naval Research 800 North Quincy St., Arlington, Virginia 22217	13. NUMBER OF PAGES 35 <i>(12) 49/</i>	
16. DISTRIBUTION STATEMENT (of this Report) Approved for public release; distribution unlimited	15. SECURITY CLASS. (of this report) Unclassified	
17. DISTRIBUTION STATEMENT (of the abstract entered in Block 20, if different from Report) Approved for public release; distribution unlimited.	18a. DECLASSIFICATION/DOWNGRADING SCHEDULE	
18. SUPPLEMENTARY NOTES Prepared in co-operation with Dominique Teillet-Billy, Laboratoire des Collisions Universite Paris-Sud, Orsay, France. Results presented at the Symposium on Negative Ions", La Mansion, Mexico, April 1981 (sponsored by NSF).	19. KEY WORDS (Continue on reverse side if necessary and identify by block number) Cl <sup>-</sup> production; dissociative attachment; negative ions; electron-molecule interaction. <i>58 41616</i>	
20. ABSTRACT (Continue on reverse side if necessary and identify by block number) Dissociative attachment H Cl + e → H + Cl <sup>-</sup> is shown to occur with cross-sections of order 1 angstrom <sup>2</sup> or larger only at impact energies within less than about 1 ev of the threshold. Cross-sections for DA are calculated for initial vibrational and rotational states populated significantly at temperatures up to 1200 deg K. The calculated cross-sections reproduce the observed result that raising the initial vibrational level from v=0 to v=2 raises the cross section by a factor of several hundred. The energy dependence of the cross-section for DA to molecules at temperatures	(cont'd)	

SECURITY CLASSIFICATION OF THIS PAGE (When Data Entered)

up to 1200 deg K agrees in orders of magnitude with experiment for both  
HC1 and DC1.

41

Accession For	
NTIS	GRA&I <input checked="" type="checkbox"/>
DTIC TAB	<input type="checkbox"/>
Unannounced	<input type="checkbox"/>
Justification	
By	
Distribution/	
Availability Codes	
Dist	Avail and/or Special
A	

S/N 0102-LF-014-6601

SECURITY CLASSIFICATION OF THIS PAGE (When Data Entered)

## CALCULATIONS ON DISSOCIATIVE ATTACHMENT TO H-CL.

### Abstract.

Dissociative attachment  $H\text{Cl} + e \rightarrow H + Cl^-$  is shown to occur with cross-sections of order 1 angstrom<sup>2</sup> or larger only at impact energies within less than about 1 ev of the threshold. Cross-sections for DA are calculated for initial vibrational and rotational states populated significantly at temperatures up to 1200 deg K. The calculated cross-sections reproduce the observed result that raising the initial vibrational level from  $v=0$  to  $v=2$  raises the cross-section by a factor of several hundred. The energy dependence of the cross-section for DA to molecules at temperatures up to 1200 deg K agrees in orders of magnitude with experiment for both HCl and DCl.

## CALCULATIONS ON DISSOCIATIVE ATTACHMENT OF ELECTRONS TO H-Cl.

### #1. Introduction.

The object of the contract was to calculate the cross-section for the reaction  $e + HCl \rightarrow H + Cl^-$  at impact energies below 5 eV. The effect of an initial vibrational excitation of the molecule was to be studied; initial levels between  $v=0$  and  $v=5$  have been considered. As a byproduct, we have calculated vibrational excitation cross-sections for molecules in different initial states.

The physical principles and the method of calculation are described in #2. The theory is tested by comparison with the available experimental data in #3. The remainder of the calculated cross-sections is given in #4. #5 is a short summary.

Some important magnitudes:

Vibrational quantum in  $HCl=0.371$  ev, in  $DCl=0.259$  ev.

Dissociation threshold of cold  $HCl=0.81$  ev, of cold  $DCl=0.87$  ev.

### #2. Physical Principles and method of calculation.

#### #2.1 The model.

The observed cross-sections for dissociative attachment to the molecule in the state  $v=0$  are shown in Fig.1 (ref.1). Evidently there is only a single peak at impact energies below 5 eV. Fig.2 shows the results of published ab initio calculations of the states of  $HCl$  and  $HCl^-$  (refs.2,3); it appears that the peak in Fig.1 between 1 and 2 eV has to be associated with a single state which dissociates into  $H + Cl^-$ . We have assumed that this state is also the one responsible for the peak in the observed cross-section for vibrational excitation below 1, which is shown in Fig.3a (ref.4).

The calculations done under the contract were based on a model which had previously led to the results marked 'calculated' in Fig.3b (ref.5). The model is defined by the following points (i)-(vi):

(i) The electron is treated as free outside the molecule. The interaction with the tail of the dipole potential is neglected because this interaction had only a negligible effect in the calculation of vibrational excitation in ref.5.

(ii) Inside the molecule, the electron is fast compared with the nuclei, even when the kinetic energy of the electron outside is only a few millivolts; therefore the wavefunction of the electron follows the nuclei adiabatically inside the molecule, so that the logarithmic derivative at the molecular surface is a function of the positions of the nuclei, and independent of the nuclear velocities.

(iii) Outside the molecule, the wavefunction of the extra electron may be expressed as a superposition of eigenstates of the angular momentum; the different  $l$ -values are coupled at the molecular surface by the asymmetry of the potential. At energies below 5 eV, the radial wavefunctions associated with the different  $l$ -values are small close to the molecule because of the centrifugal potential barriers. The value  $l=0$  is an exception, so that its contribution to the scattering is dominant at energies below 5 eV. Only the s-wave is taken into account when the electron is outside the molecule. This approximation is consistent with the spherical symmetry of the observed angular distribution of scattered electrons in vibrational excitation below 1 eV (ref.4).

(iv) The energies of interest are sufficiently low for the logarithmic derivative of the radial function in the s-wave at the molecular surface to be treated as independent of energy, because the varying kinetic energy of the electron outside the molecule is much smaller than the depth of the potential inside. The logarithmic derivative of the s-wave at the molecular surface may be written  $f_0 + f_1(R-R_0)$ , where  $R$  is the nuclear separation, and  $R_0$  the value of  $R$  at equilibrium.  $f_0$  and  $f_1$  are constants, determined from a fit of the observed cross-sections for vibrational excitation (ref.5). The linear approximation with respect to  $(R-R_0)$  is justified for vibrational excitation, where the excursion of the nuclei from equilibrium is much smaller than one bohr ( $=0.52$  angstrom) during the collision, because in the absence of a trapping mechanism, the collision does not involve any time delay. (In point (v) below, we shall return to the range of validity of the linear approximation.)  $f_1$  is of order unity because the interior electronic wavefunction changes by a substantial fraction of itself when  $R$ , the nuclear separation, changes by one bohr; we have used the value 0.45 in our calculations.  $f_0$  is close to zero, with a fitted value of 0.075; (this value is appropriate if the logarithmic derivative refers to  $(r \times s\text{-wave})$ , rather than to the s-wave without the factor  $r$ , as in ref.5).

The small value of  $f_0$  implies that the s-wave of the electron for nuclei fixed at their equilibrium positions is approximately  $r[\cos(kr)/(kr)]$ , instead of  $r[\sin(kr)/(kr)]$  as in the incident plane wave. Thus the wavefunction of the electron close to the molecule is greatly enhanced relative to the incident plane wave; this enhancement is responsible for the very large cross-section for vibrational excitation near threshold (see Fig.3).

(v) The potential for the negative ion can be calculated from the parameters  $f_0$  and  $f_1$ , the binding energy being  $(f_0 + f_1(R-R_0))^2/2$ ; the result is shown in Fig.4. The potential corresponding to the fitted logarithmic derivative is the curve marked  $H^-Cl^-$ , which leaves the curve  $H^-Cl$  at  $R_s=2.58$  bohr, and runs to the point A. The fit of the vibrational excitation is sensitive to the potential only close to the equilibrium separation; however, the linear approximation must be quite good out to A because the fit of the transition  $v=0 \rightarrow v=2$  is satisfactory in ref.5; the  $v=2$  vibrational level has its turning-point 0.45 bohr to the right of the equilibrium.

There cannot be a barrier beyond A, because dissociative attachment is observed to set in strongly at threshold (ref.1); therefore the potential must turn over near A to a nearly horizontal curve, as shown in Fig.4. The resultant potential, represented by the complete curve marked H Cl- in Fig.4, is not very different from the calculated H Cl- potentials given in refs.2 and 3.

(vi) For dissociative attachment, we assumed that the transition to the bound H Cl- state is driven by the non-adiabatic coupling of the extra electron to the velocities of the nuclei (Fig.5). In other words, the electron is captured into the bound state to the right of  $R_s$  in Fig.5, by transferring its binding energy to the nuclei. This mechanism is quite different from the familiar mechanism of dissociative attachment at a quasistationary state, where the potential curve for the negative ion continues from the region of finite binding for the extra electron into the region of positive energies; here attachment starts when the electron tunnels into the molecule in a manner which does not depend on the nuclear velocities. In the absence of a trapping mechanism at positive energies for the extra electron, there is no localised electronic state which one might associate an H Cl- ion when  $R < R_s$ .

## #2.2 Method of calculation.

A wavefunction which includes dissociative attachment may be written

$$\Psi(r, R) = \varphi(r, R) \xi(R) + \Psi'(r, R), \quad (1)$$

where  $\varphi$  is the bound H Cl- eigenfunction of the electronic Hamiltonian; it belongs to the eigenvalue  $E_0(R)$ .  $\xi(R)$  is the associated nuclear wavefunction of the negative ion. One may write

$$\xi(R) = (\varphi | \Psi)_{\epsilon}, \quad (2)$$

where the notation  $(\dots | \dots)_{\epsilon}$  means that the integral extends over the electron co-ordinates while the nuclei are held fixed.  $\Psi'$  is the part of the wavefunction orthogonal to  $\varphi$  in the space of electron co-ordinates. One has  $\xi(R_s) = 0$  because  $\varphi(r, R_s) = 0$  at all finite distances of the electron when  $R = R_s$  in Fig.4, due to the infinite radial extent when the binding energy vanishes.

If one inserts  $\Psi$  into the Schrödinger equation, multiplies by  $\varphi$ , and integrates over the co-ordinates of the electrons, one obtains the nuclear wave-equation for the negative ion:

$$-\frac{1}{2M} \frac{\partial^2 \xi}{\partial R^2} + [E_0(R) - E] \xi - \frac{1}{M} (\varphi | \frac{\partial \varphi}{\partial R})_{\epsilon} \frac{\partial \xi}{\partial R} - \frac{1}{2M} (\varphi | \frac{\partial^2 \varphi}{\partial R^2})_{\epsilon} \xi = \frac{1}{2M} (\varphi | \frac{\partial^2}{\partial R^2} \Psi')_{\epsilon}. \quad (3)$$

There cannot be a barrier beyond  $A$ , because dissociative attachment is observed to set in strongly at threshold (ref.1); therefore the potential must turn over near  $A$  to a nearly horizontal curve, as shown in Fig.4. The resultant potential, represented by the complete curve marked  $H\text{Cl}^-$  in Fig.4, is not very different from the calculated  $H\text{Cl}^-$  potentials given in refs.2 and 3.

(vi) For dissociative attachment, we assumed that the transition to the bound  $H\text{Cl}^-$  state is driven by the non-adiabatic coupling of the extra electron to the velocities of the nuclei (Fig.5). In other words, the electron is captured into the bound state to the right of  $R_s$  in Fig.5, by transferring its binding energy to the nuclei. This mechanism is quite different from the familiar mechanism of dissociative attachment at a quasistationary state, where the potential curve for the negative ion continues from the region of finite binding for the extra electron into the region of positive energies; here attachment starts when the electron tunnels into the molecule in a manner which does not depend on the nuclear velocities. In the absence of a trapping mechanism at positive energies for the extra electron, there is no localised electronic state which one might associate an  $H\text{Cl}^-$  ion when  $R < R_s$ .

## #2.2 Method of calculation.

A wavefunction which includes dissociative attachment may be written

$$\Psi(r, R) = \varphi(r, R) \xi(R) + \Psi'(r, R), \quad (1)$$

where  $\varphi$  is the bound  $H\text{Cl}^-$  eigenfunction of the electronic Hamiltonian; it belongs to the eigenvalue  $E_o(R)$ .  $\xi(R)$  is the associated nuclear wavefunction of the negative ion. One may write

$$\xi(R) = (\varphi | \Psi)_{\text{e}}, \quad (2)$$

where the notation  $(\dots | \dots)_{\text{e}}$  means that the integral extends over the electron co-ordinates while the nuclei are held fixed.  $\Psi'$  is the part of the wavefunction orthogonal to  $\varphi$  in the space of electron co-ordinates. One has  $\xi(R_s) = 0$  because  $\varphi(r, R_s) = 0$  at all finite distances of the electron when  $R = R_s$  in Fig.4, due to the infinite radial extent when the binding energy vanishes.

If one inserts  $\Psi$  into the Schrödinger equation, multiplies by  $\varphi$ , and integrates over the co-ordinates of the electrons, one obtains the nuclear wave-equation for the negative ion:

$$-\frac{1}{2M} \frac{\partial^2 \xi}{\partial R^2} + [E_o(R) - E] \xi - \frac{1}{M} (\varphi | \frac{\partial \varphi}{\partial R} ) \frac{\partial \xi}{\partial R} - \frac{1}{2M} (\varphi | \frac{\partial^2 \varphi}{\partial R^2} )_{\text{e}} \xi = \frac{1}{2M} (\varphi | \frac{\partial^2}{\partial R^2} \Psi' )_{\text{e}}. \quad (3)$$

$M$  is the reduced mass of the nuclei. One has

$$(\varphi | \frac{\partial \varphi}{\partial R})_e = 0 \quad (4)$$

because  $(\varphi | \frac{\partial \varphi}{\partial R})_e = 1$ , because of the normalisation. The non-adiabatic term  $(\varphi | \frac{\partial \varphi}{\partial R})_e$  is small compared with the kinetic energy term  $\frac{\partial^2 \varphi}{\partial R^2}$  because  $\varphi$  varies slowly with  $R$  in comparison with  $\frac{\partial \varphi}{\partial R}$ ; this non-adiabatic term was dropped.

The amplitude of  $\xi$  when  $R \rightarrow \infty$  is given by

$$\xi \rightarrow e^{i(KR+\delta)} \int_{R_s}^{\infty} dR' \left\{ 2 \frac{\partial u^0}{\partial R} \frac{\partial}{\partial R'} (\varphi_1 + u^0(R') \frac{\partial^2}{\partial R'^2} (\varphi_1)) \right\} |\Psi'\rangle_e \quad (5)$$

The function  $u^0(R)$  is the solution of the homogeneous version of the nuclear wave-equation, which satisfies  $u^0(R_s) = 0$ , and behaves asymptotically like  $u^0(R) \rightarrow \sin(KR + \delta)$ .  $K$  is given by  $K = [2(E_0(\infty) - \varepsilon)M]^{1/2}$ . The derivation uses the boundary conditions  $\xi \rightarrow \text{const.} e^{iKR}$  as  $R \rightarrow \infty$ , and  $\varphi(r, R_s) = 0$ . In the calculations under the contract, the integral  $\int dR \dots$  was worked out with the asymptotic form for the electronic wavefunction  $\varphi$ , because most of the transition must occur at small binding energies, where the radial extent of the electronic wavefunction is very large compared with the target. The second order term containing  $\frac{\partial^2 \varphi}{\partial R^2}$  was dropped.

For the function  $\Psi'$ , we used the wavefunction determined by the solution of the boundary condition

$$[f_0 + (R - R_s) f_1] \Psi'(r_s, R) = 0, \quad (6)$$

at the molecular surface  $r_s$ , by an expansion of the wavefunction in vibrational eigenfunctions of the neutral molecule. (That expansion yields the vibrational excitation.) Nine vibrational levels were taken into account; this number was chosen after some tests to check on convergence. The boundary condition was applied at  $r_s = 0$ , because the wavefunction of the electron outside the molecule varies on a scale large compared with the size of the molecule.

A peculiar difficulty arises in the calculation of this approximation for  $\Psi'$ . Because the tails of the vibrational wavefunctions in the neutral stick out into the region in Fig.4 where the  $\text{HCl}^-$  potential lies below the  $\text{HCl}$  potential, there are quasistationary states due to the attachment of an electron to the excited vibrational levels; such states are sometimes called 'nuclear excited Feshbach resonances'. The resonances of this kind which are associated with the levels  $v=1$  and  $v=2$  are probably genuine physical phenomena (ref.6); they lie below the threshold for dissociation into  $\text{H} + \text{Cl}^-$ , so that the emission of an electron is their only mode of decay. However, if one uses the potential for  $\text{HCl}^-$  associated with the linear approximation for the logarithmic derivative, then the part of the  $\text{HCl}$  potential which extends beyond the point A in Fig.4 gives rise to quasistationary states due to the attachment of an electron to the  $\text{HCl}$  levels from  $v=3$  upwards, in addition to

the levels below  $v=3$ . But the higher levels are artifacts, because the approximation for the HCl- potential from the linear logarithmic derivative does not allow them to decay by dissociation, which is now energetically possible. If one calculates the function  $\Psi'$  in the manner of ref.5, with the linear approximation for the logarithmic derivative, then it resonates at the artificial resonances. The artificial resonances lie too high to affect the vibrational excitation in the threshold region discussed in ref.5, but they introduce very serious errors in the dissociative attachment which occurs above the dissociation threshold.

A really satisfactory treatment of the artificial resonances was not possible within the limited scope of this contract. What is needed is a calculation of the vibrational excitation and dissociative attachment simultaneously, with a final-state potential for HCl- which reproduces the dissociation energy. In such a treatment, the artificial resonances would be destroyed by dissociation. However, that would be a much more ambitious calculation than the treatment of dissociative attachment as a perturbation on vibrational excitation, which is what I had planned for this contract. I intend to continue working on the more ambitious theory, but for the present, I have used a 'crutch' to get rid of the artificial resonances. The crutch retains the linear approximation for the logarithmic derivative to calculate the function  $\Psi'$ , but drops the contribution of any vibrational state of HCl from the function  $\Psi'$  whenever the total energy is not more than 100 mev below that state. This trick never drops more than a few of the levels contributing to the function  $\Psi'$ , because the spacing of the vibrational levels is 350 meV, and because the different rotational sublevels of any vibrational level differ by up to about 200 meV in rotational energy. The accuracy of the results can be judged by comparison with the limited available measurements; (see #4).

### #3. Tests of the theory: Comparison with observations.

#### #3.1 Vibrational Excitation.

Our calculated results for vibrational excitation near threshold are shown in Fig.3b. Fifteen vibrational levels of HCl were included in the calculation. (The calculations on DA used 9.) There is nothing novel about these results; they merely show that the programs used for the present calculations were at least as good at calculating vibrational excitation as the one's Dube and I used four years ago on the same problem in ref.5.

The calculation uses a harmonic oscillator model.

#### #3.2 Dissociative Attachment.

The calculation of dissociative attachment sketched in the previous paragraph uses the wavefunction behind the results in Fig.3 to evaluate the integral in eq.5. In addition to this wavefunction, one needs a potential for the nuclei in the negative ion. We used the potential in Fig.4; at separations smaller than the point A, it follows from the linear approximation for the logarithmic derivative in equ.6. The point A was chosen so that the potential is 0.05 ev below the asymptotic limit. From A, the potential was joined smoothly to the polarisation potential of an H atom near the single charge of the Cl- ion at large separations. The rest of the calculation involves no further' adjustments of physical parameters.

The calculation was done for different initial angular momenta and vibrational states of the nuclei, up to  $l=18$  and  $v=2$  for HCl and up to  $l=27$  and  $v=4$  for DC1. (As we said before, 9 vibrational levels were included in the calculation. The limiting values were chosen to reach all the angular momentum states populated significantly at temperatures up to 1200 deg K.) The angular momentum of the nuclei comes entirely from the initial molecular state, because the electron is presumed to enter in an s-state.

The available experimental measurements for  $HCl + e \rightarrow H + Cl^-$  at temperatures up to 1200 degrees K are shown in Fig.6a, taken from a recent paper(7). The corresponding calculated results are shown in Fig.6b; these curves were obtained by a Boltzmann average of the calculated results for different initial  $l$  and  $v$  for the molecule. The electron impact energy was varied in steps of 50 mev; each cross-section was smeared out over its 50 mev interval in the pictures.

It is important that any initial excitation energy of the molecule, in vibration or rotation, contributes to the dissociation energy. Therefore the dissociative attachment thresholds for the excited states are lower than the threshold for the ground state by the initial excitation energy. The threshold in HCl is 0.81 ev for the ground state ( $v=0, l=0$ ), and 0.44 ev and 0.07 ev for ( $v=1, l=0$ ) and ( $v=2, l=0$ ). The difference in thresholds makes it easy to identify the contribution of excited states in Fig.6 near their thresholds. Since the mean rotational kinetic energy is only 0.1 ev at 1000 deg K, the strong cross-sections in Fig.6 well below the cold threshold at 0.81 ev must involve initial vibrational excitation.

The most striking aspect of the results in Fig.6 is the important contribution of the excited vibrational states of the target. Because of the low population of the state  $v=2$  in HCl, the dissociative attachment cross-sections to the state  $v=2$  must be a few hundred times larger than the cross-sections for  $v=0$  to show as large in the experimental curves as it does. The theory reproduces the relative importance of the higher  $v$  levels in reasonable agreement with experiment. There is also an indication of an enhancement of the cross-sections by rotational excitation in the molecule, when the rotational kinetic energy lowers the DA threshold through one of the vibrationally excited target states. This enhancement is again reproduced fairly well by the theory. (The peak marked '3' on the calculated curve for 1180 deg K is due to this effect.) The mechanism of this effect is not completely understood.

Fig.7 shows the observed and calculated cross-sections for DA in DCI at 1140 deg K (observations from ref.7). There is again a very large contribution from the vibrationally excited states of the target, whose relative magnitude is reproduced by the calculation.

The experimental measurements in Fig.6a and Fig.7 are not absolute. The only absolute measurements available are those shown in Fig.1, for DA to cold HCl and DCI. These results are compared with the calculations in Fig.8, where the points indicate the experiments, and the continuous curve the theory. The calculation lies between a factor 2 and 3 above the experiments, even after one allows for a smoothing out of the structure in the calculated results. This discrepancy in the absolute magnitude is the major failure of the theory. However, the ratio of the cross-sections for HCl and DCI in Fig.8 is correct in the theory.

#### #4. Calculated cross-sections for individual channels.

The calculated cross-sections for different initial and final channels are shown in Fig.9 for vibrational excitation, and in Fig.10 for dissociative attachment. These are the cross-sections which are combined in Figs.3,6, and 7 with Boltzmann weighting factors.

Our model neglects coupling between vibrations and rotations, so that the rotations enter only through their kinetic energy.

An examination of the calculated cross-sections shows that they do not satisfy the detailed balance theorem exactly. Generally, and particularly for the larger cross-sections, the ratio of inverse cross-sections lies within a factor 1.5 of the value required by detailed balancing. The origin of this difficulty is that the calculation treats dissociative attachment as a perturbation on vibrational excitation; one would have to treat the two processes in a more symmetric manner to satisfy detailed balancing.

## #5. Summary and conclusion.

We conclude:

The model which accounted for vibrational excitation of HCl in the threshold region in ref.5 accounts also for the following aspects of dissociative attachment  $HCl + e \rightarrow H + Cl^-$ :

(1) The dependence on energy ; in particular, the model suggests that the production of  $Cl^-$  ions should occur only at electron impact energies within one ev of the threshold.

(2) The ratios of the cross-sections for different initial vibrational and rotational states; in particular, the model predicts an increase of a factor of several hundred in the cross-section when the molecule is raised from the vibrational ground-state to the second vibrational excited state.

(3) The ratios of the cross-sections for  $HCl + e \rightarrow H + Cl^-$  and  $DCl + e \rightarrow D + Cl^-$ ; in particular, the model suggests that for the lowest vibrational state, the cross-section should be about five times smaller for  $DCl$  than for  $HCl$ .

The model gives DA cross-sections too large in absolute magnitude by a factor of 2-3 in the only case where measurements have been made, for molecules with no vibrational excitation.

The calculations do not satisfy detailed balancing exactly, essentially because they treat dissociative attachment as a perturbation on vibrational excitation. For the larger cross-sections, the ratio of the cross-sections for inverse processes generally lies within a factor 1.5 of the value required by detailed balancing.

The calculations show that the DA cross-sections fall rapidly as the energy rises above threshold, within about one ev or a little less. Together with the fact that there is only a single state available for the dissociation into  $H + Cl^-$ , according to refs.2 and 3, this rapid fall-off shows that the threshold peaks of dissociative attachment we have calculated are the only contribution to dissociative attachment at impact energies below 5 ev.

Acknowledgement. This work was done in collaboration with Dominique Teillet-Billy, of the Laboratoire des Collisions, Batiment 351, Universite Paris-Sud, Orsay, France.

References.

- (1) R.Azria, L.Roussier, R.Paineau, and M.Tronc,  
Rev.Phys.Appl., Paris, 9,469,1974.
- (2) H.S.Taylor, E.Goldstein, G.A.Segal, J.Phys.B, 10,2253,1977.  
E.Goldstein, G.A.Segal, and R.W.Wetmore, J.Chem.Phys. 68,271,1978.
- (3) M.Krauss and W.J.Stevens, J.Chem.Phys., 74,570,1981.
- (4) K.Rohr and F.Linder, J.Phys.B, 9,2521,1976.
- (5) L.Dube and A.Herzenberg, Phys.Rev.Lett., 38,820,1977.
- (6) J.P.Gauyacq and A.Herzenberg, to be published.
- (7) M.Allan and S.F.Wong, J.Chem.Phys., Feb.1981.

#### FIGURE CAPTIONS.

Fig.1. Observed cross-sections for dissociative attachment to H-Cl. (From ref.1.) The cross-section for D-Cl + e  $\rightarrow$  D + Cl- is similar in shape but smaller by a factor 5 at the threshold.

Fig.2. Ab initio calculated energy-levels for H Cl and H Cl-. (From refs. 2 and 3.)

Fig.3a. Dots: Observed cross-sections for vibrational excitation e + H Cl(v=0)  $\rightarrow$  e' + H Cl(v=1). Continuous curve: Calculated in 1977. (From ref.5. Data from ref.4.)

3b. Calculation with the present program.

Fig.4. Potential energy curves used in the present calculation. H Cl: Harmonic oscillator model.

H Cl-: Binding energy of the extra electron from the logarithmic derivative of the wavefunction which fits the vibrational excitation in Fig.3a, at separations smaller than A. At larger distances, polarisation potential.

Fig.5a. The traditional adiabatic model for dissociative attachment, where the incoming electron tunnels into a quasistationary state through a potential barrier. The nuclei then slide apart with the extra electron trapped by the barrier, until the electronic state becomes truly bound at the point  $R_s$ .

5b. The non-adiabatic model behind the present calculations. There is no barrier to hold the electron at separations smaller than  $R_s$ . An incoming electron is captured into the bound state at separations larger than  $R_s$  by the coupling to the finite velocity of the nuclei.

Fig.6a. Observed DA to H Cl at various temperatures up to 1200 deg K. (From ref.7.) The features marked in the top diagram may correspond to the features marked in Fig.6b.

6b. The present calculations of DA at the temperatures corresponding to Fig.6a.

Fig.7. Observed DA to D Cl (from ref.7), and corresponding results from the present calculation.

Fig.8. Absolute magnitudes in experiment and theory. Dots: Observations, from Fig.1 and ref.1. Continuous curve: Present calculation.

8a. H Cl.

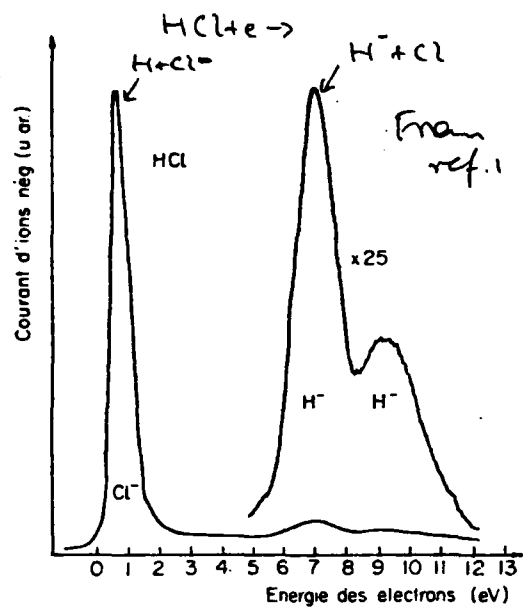
8b. D Cl.

Fig.9. The present calculations for vibrational excitation from different initial vibrational states, all for  $l=0$ .

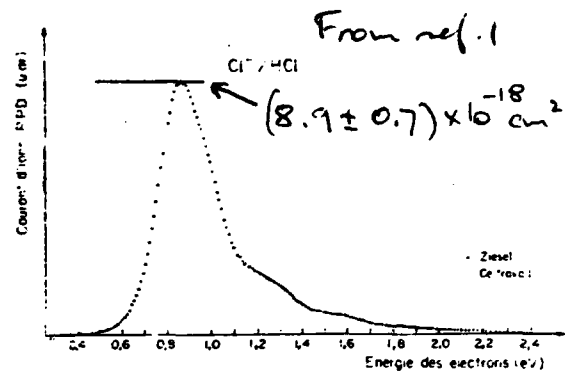
Fig. 10. The present calculations for dissociative attachment for different initial vibrational states.

10a. H Cl.

10b. D Cl.

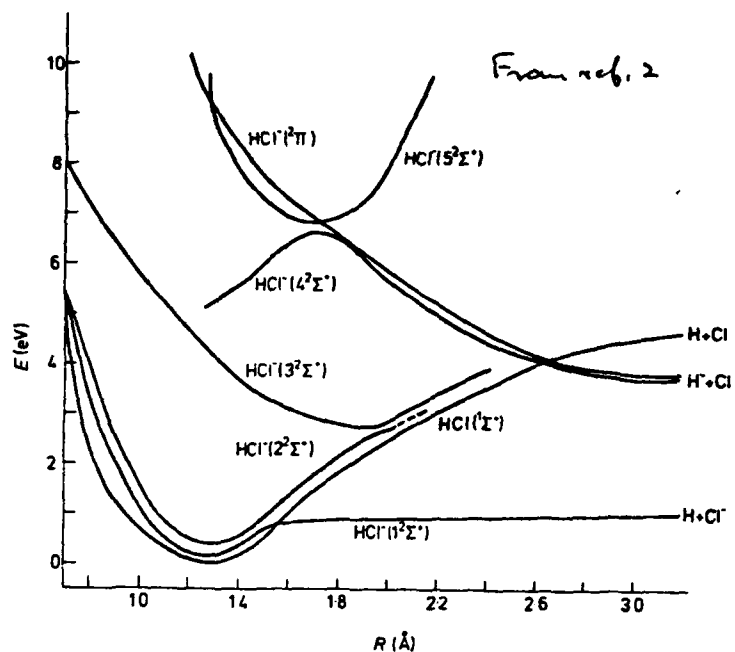


Formation d'ions négatifs par attachement dissociatif dans HCl.



— Forme du pic  $\text{Cl}^-/\text{HCl}$ . Comparaison entre nos mesures et celles de Ziesel et Schulz [12].

Fig. 1



Calculated potential energy curves for  $\text{HCl}^-$  and  $\text{HCl}$  ( $x\ 1\Sigma^+$ ).

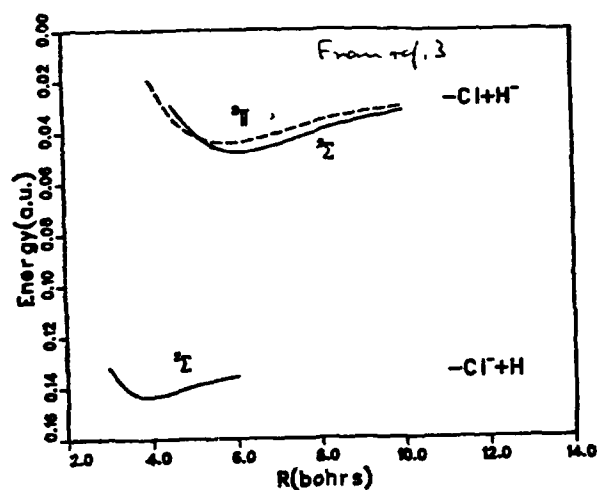


FIG. 1. The  $\text{HCl}^-$  energy curves are drawn relative to their respective experimental asymptotes  $\text{Cl}^- + \text{H}$  and  $\text{Cl} + \text{H}^-$ . The energy scale is in atomic units and is measured relative to the energy of the neutral  $\text{Cl} + \text{H}$  asymptote.

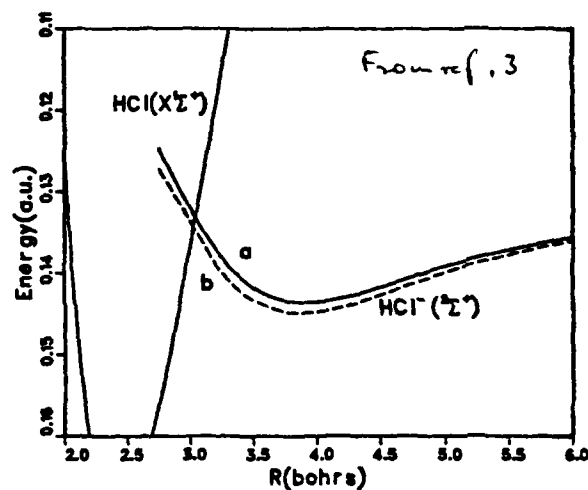


Fig. 2

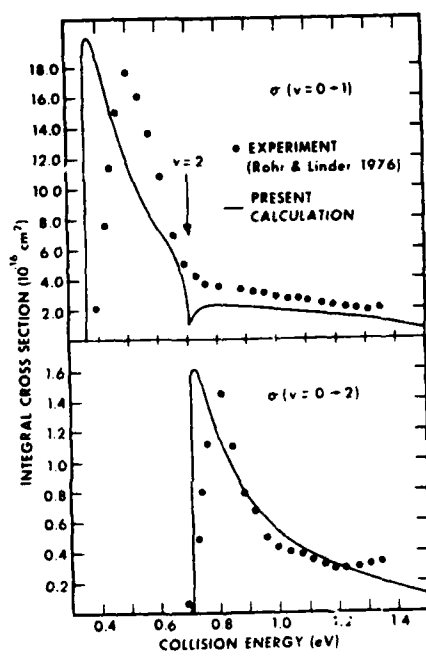
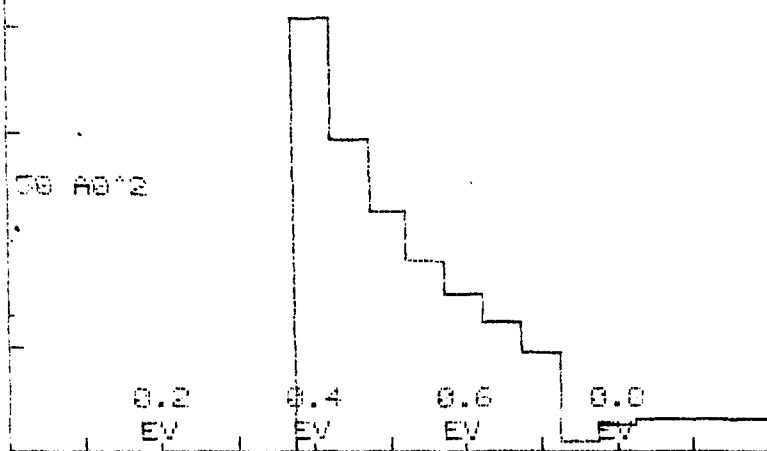


Fig. 3a

100 AG-2

INITIAL V=0



$V = 0 \rightarrow 1$

10 AG-2

INITIAL V=0

0 AG-2

$V = 0 \rightarrow 2$

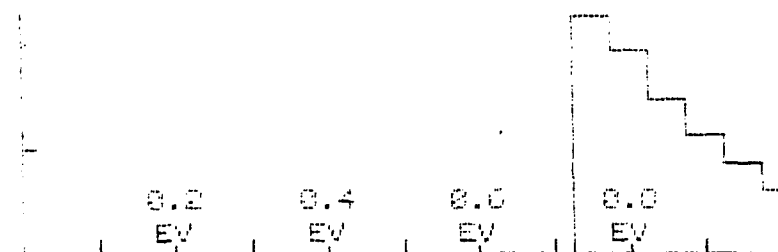


Fig. 3b

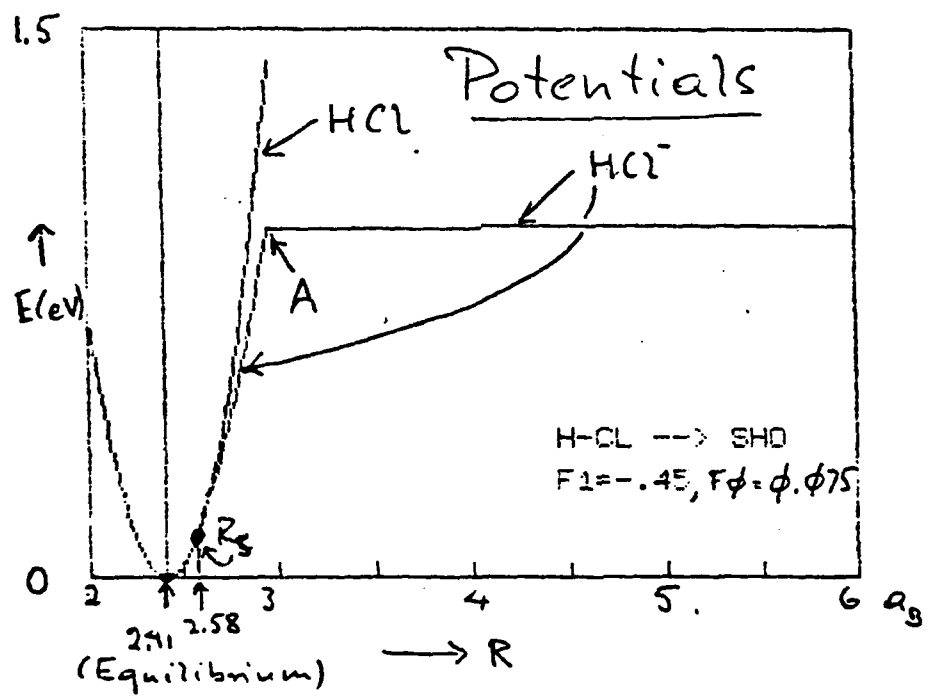


Fig. 4

Fig. 5a. Quasistationary state model.

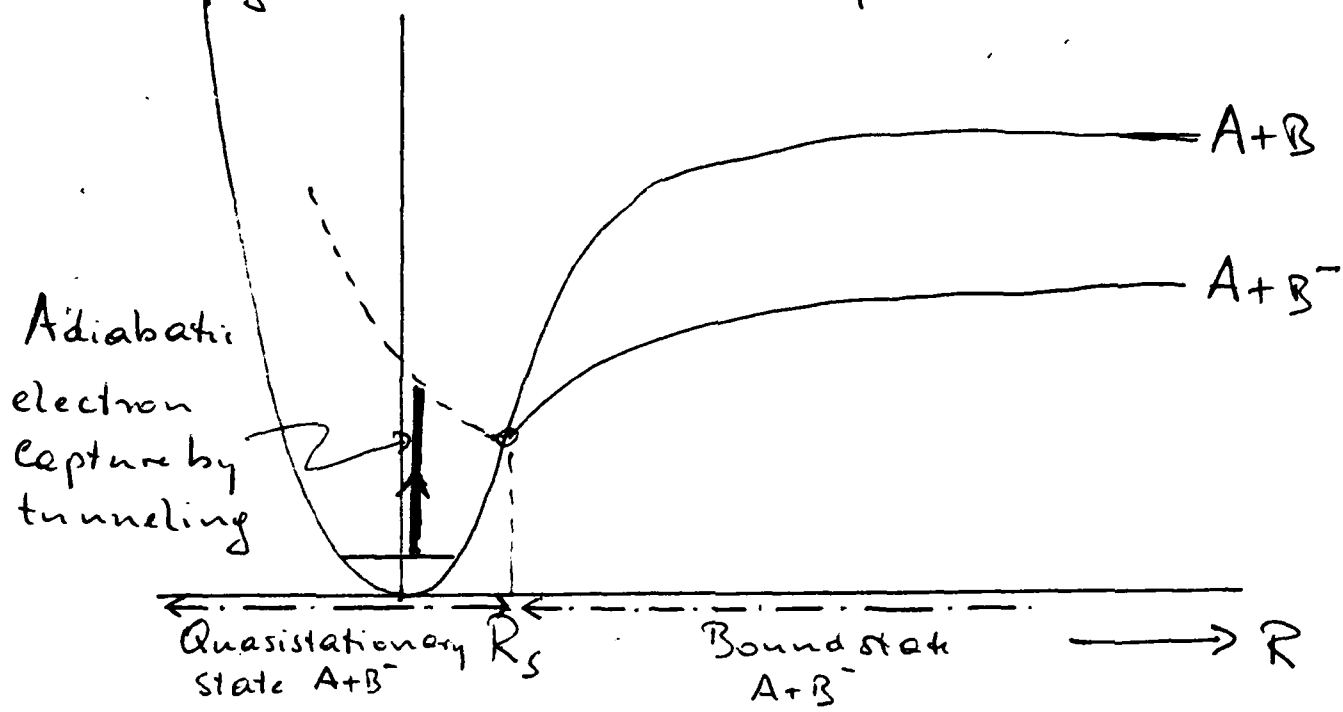
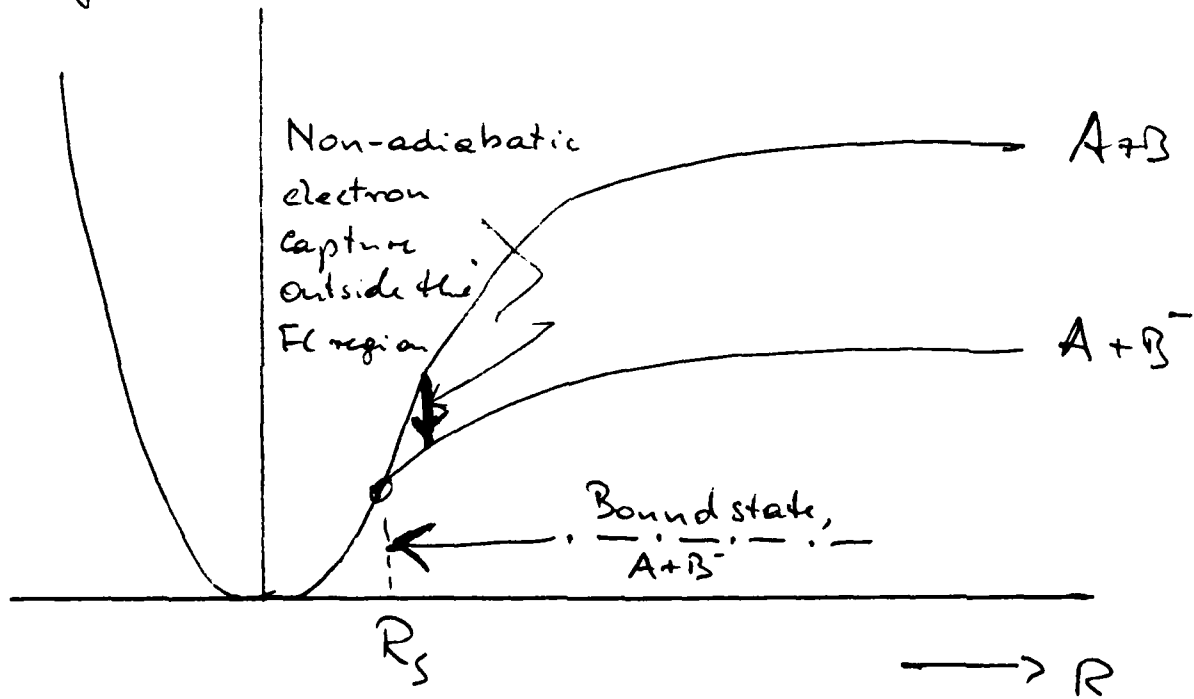


Fig. 5b. Present ('Virtual state') model.



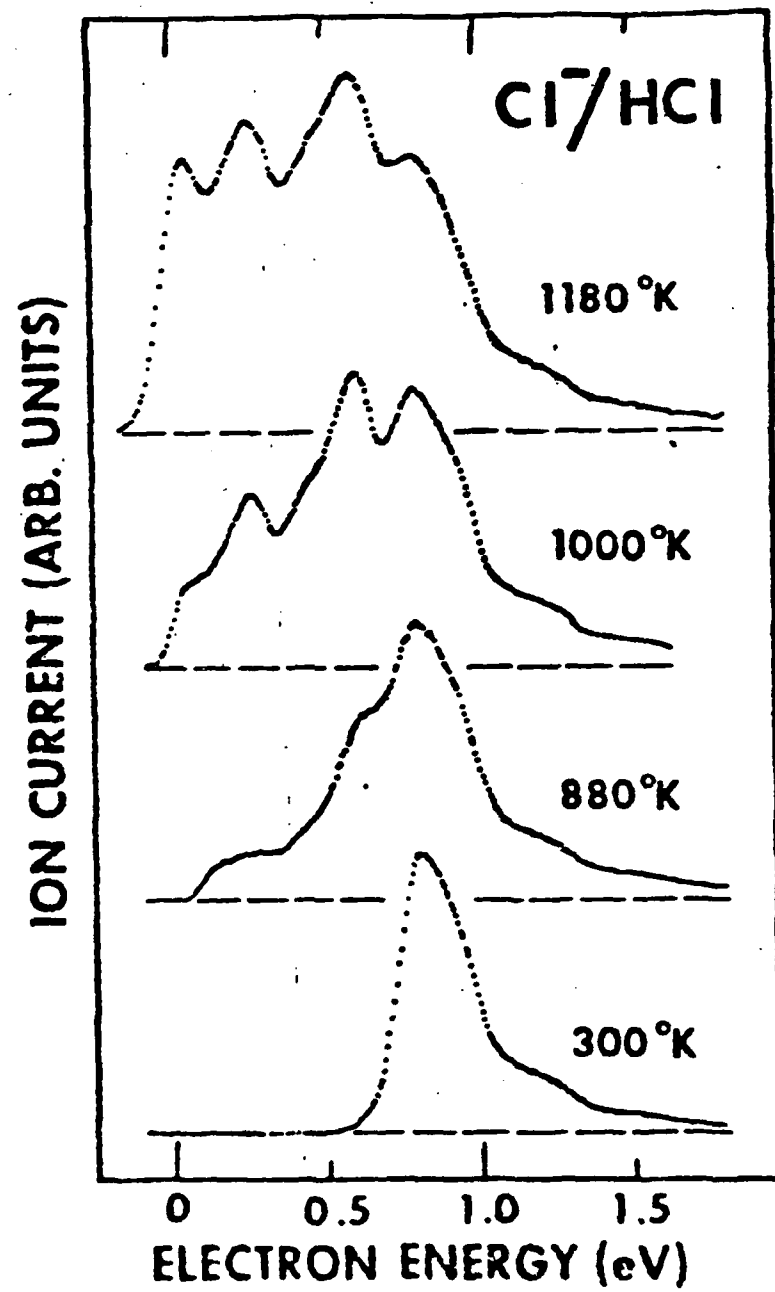
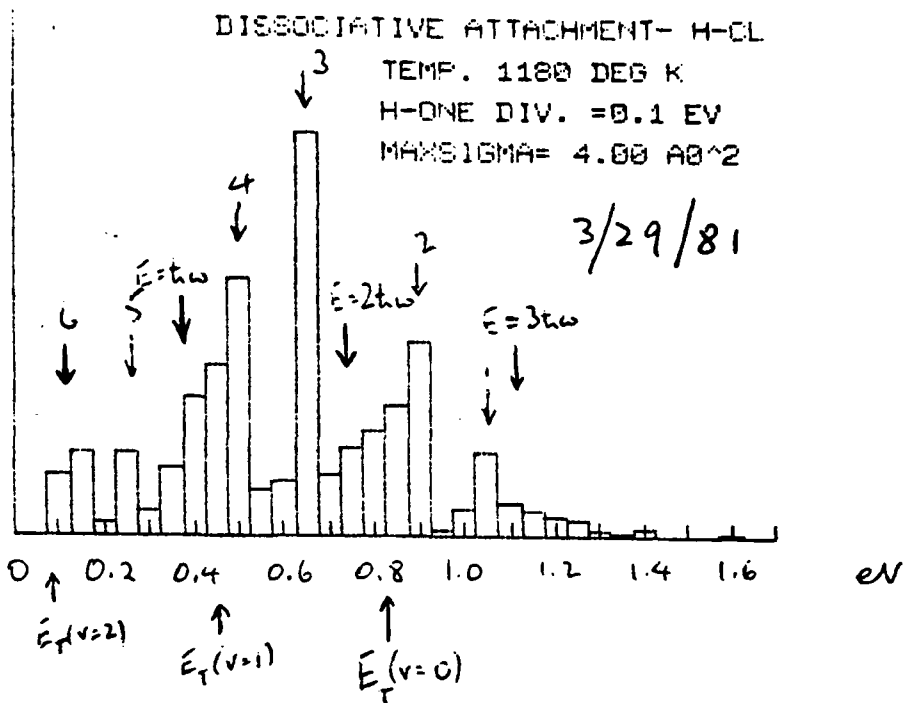


Fig. 6 a



DISSOCIATIVE ATTACHMENT- H-CL

TEMP. 1000 DEG K  
 H-ONE DIV. = 0.1 EV  
 MAXSIGMA= 4.00 A0^2

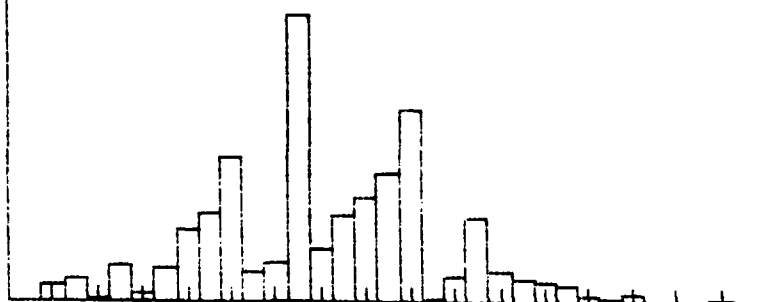


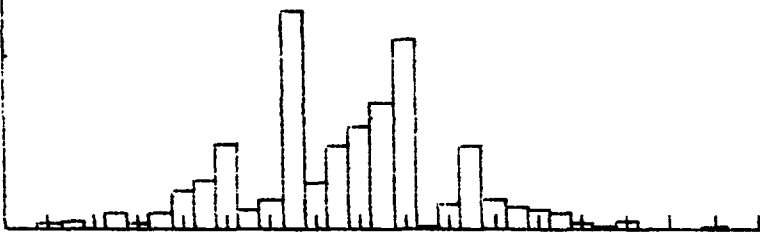
Fig. 6b

DISSOCIATIVE ATTACHMENT- H-CL

TEMP. 630 DEG K

H-ONE DIV. = 0.1 EV

MAXSIGMA= 4.00 A0^2



DISSOCIATIVE ATTACHMENT- H-CL

TEMP. 300 DEG K

H-ONE DIV. = 0.1 EV

MAXSIGMA= 4.00 A0^2

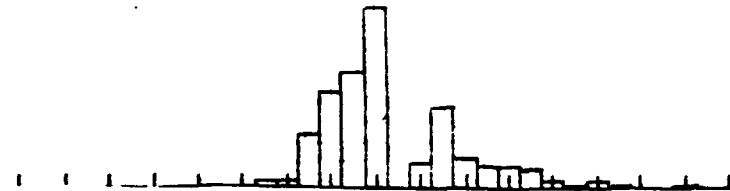
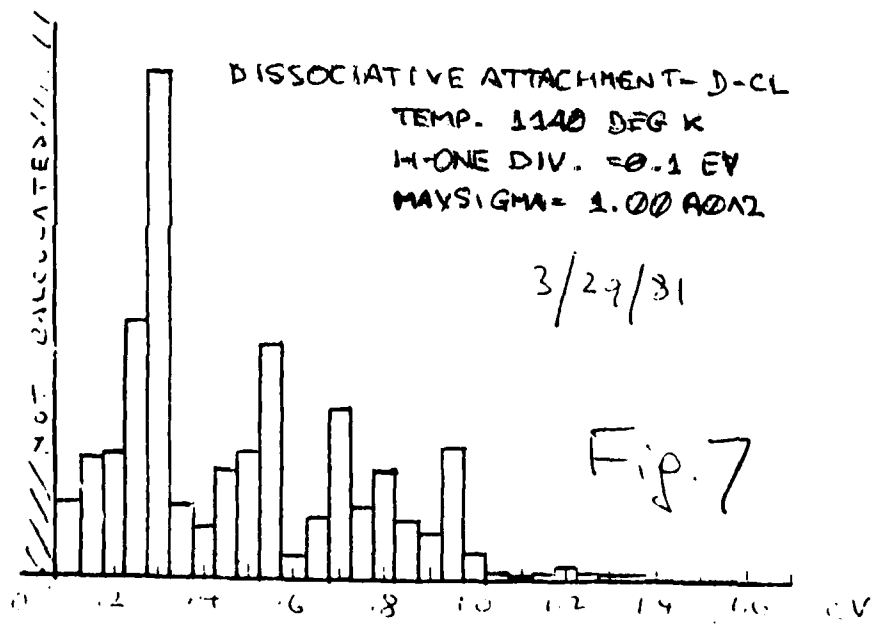
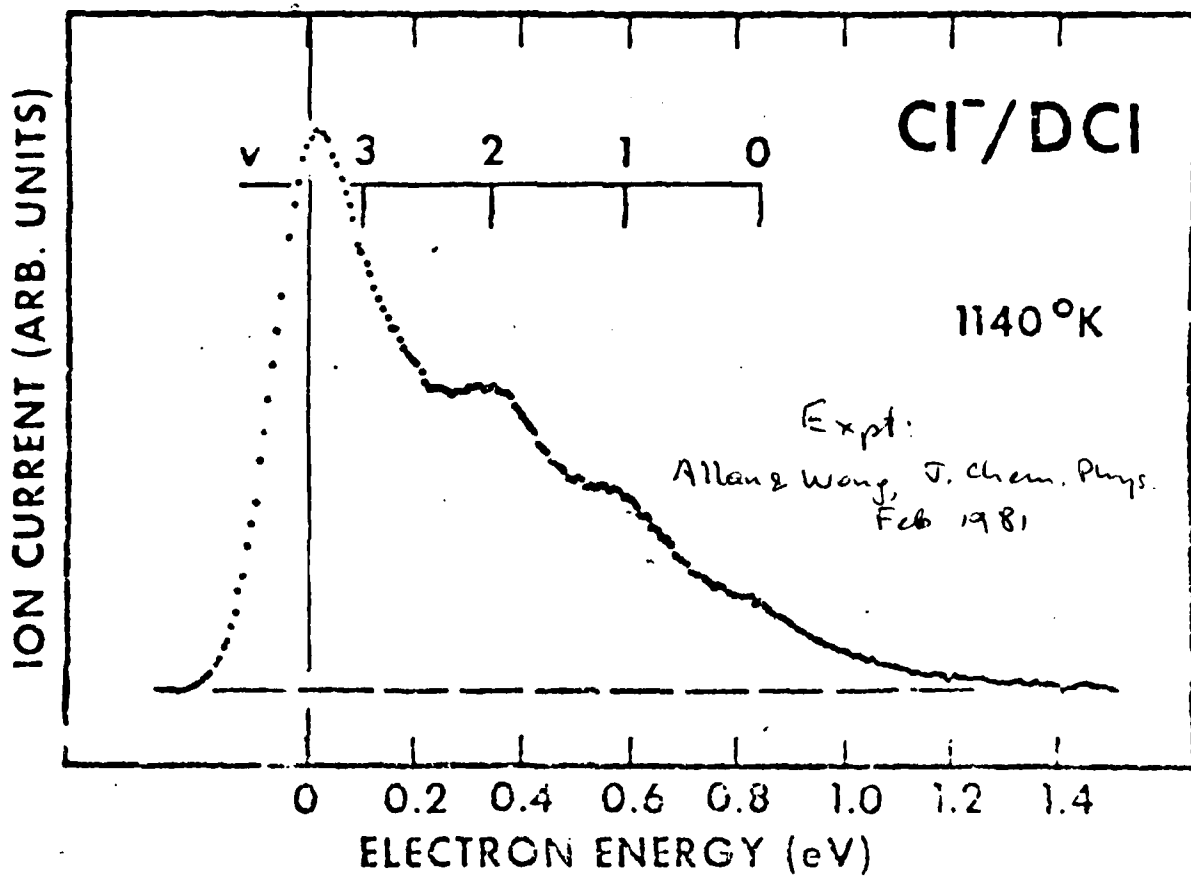


Fig. 6b

7. 1.



ONE HORIZONTAL DIV. = 0.1 EV  
VERT. AXIS = 1.58A0^2

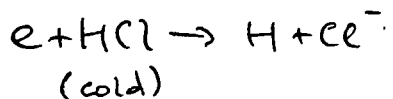
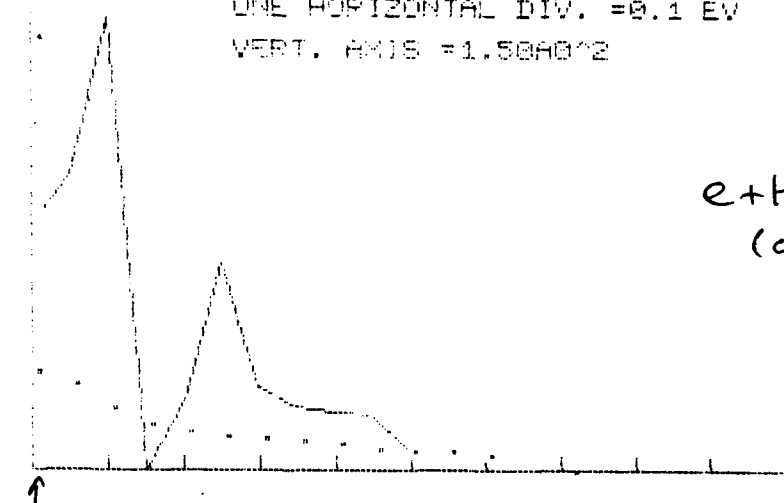


Fig. 8a

ONE HORIZONTAL DIV. = 0.1 EV  
VERT. AXIS = 0.58A0^2

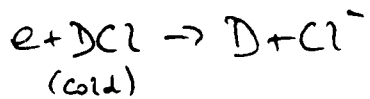
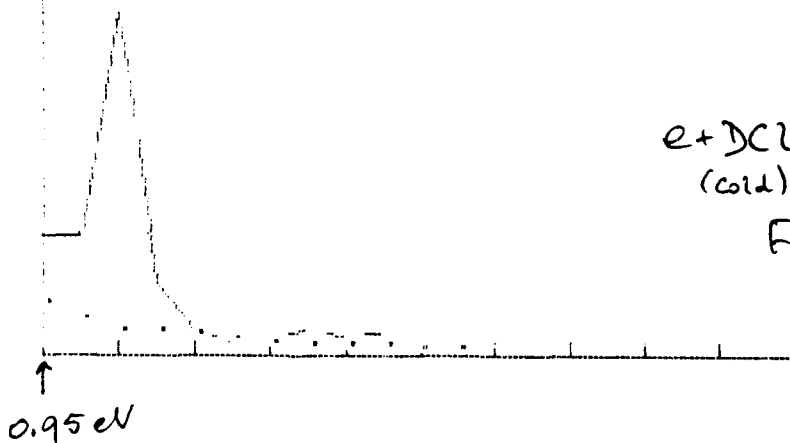


Fig. 8b

1000 AD/2

INITIAL  $V=1$

100 AD/2

$V = 1 \rightarrow \emptyset$

0.2 0.4 0.6 0.8  
EV EV EV EV

100 AD/2

INITIAL  $V=1$

50 AD/2

$V = 1 \rightarrow 2$

0.2 0.4 0.6 0.8  
EV EV EV EV

10 AD/2

INITIAL  $V=1$

$V = 1 \rightarrow 3$

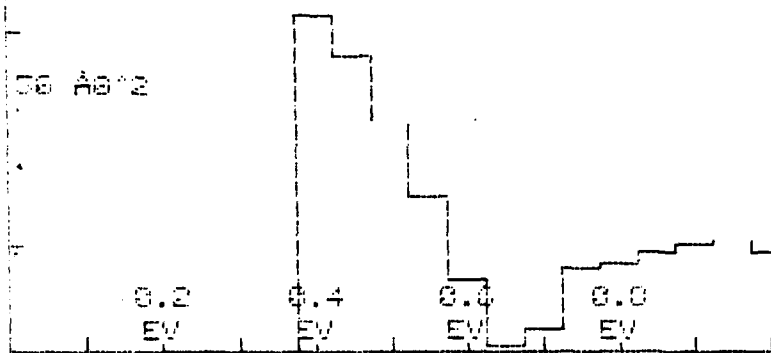
0 AD/2

0.2 0.4 0.6 0.8  
EV EV EV EV

Fig. 9

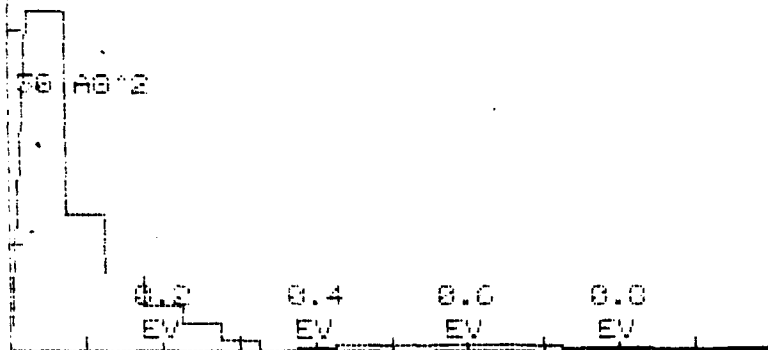
Fig. 9 cont'd

INITIAL V=2



1000 AG/2

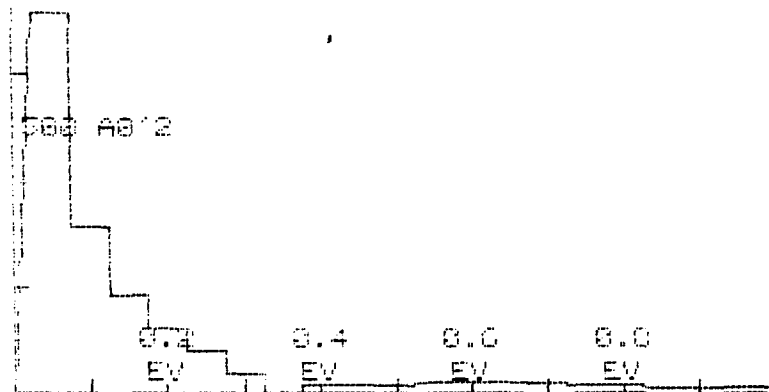
INITIAL V=2



$V=2 \rightarrow \emptyset$

1000 AG/2

INITIAL V=2

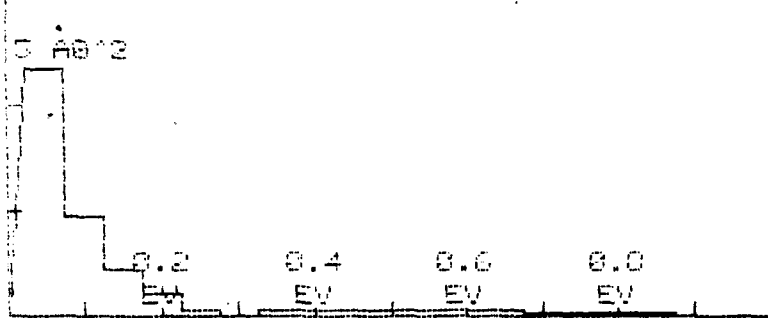


$V=2 \rightarrow 1$

Fig. 9 contd.

116 4612

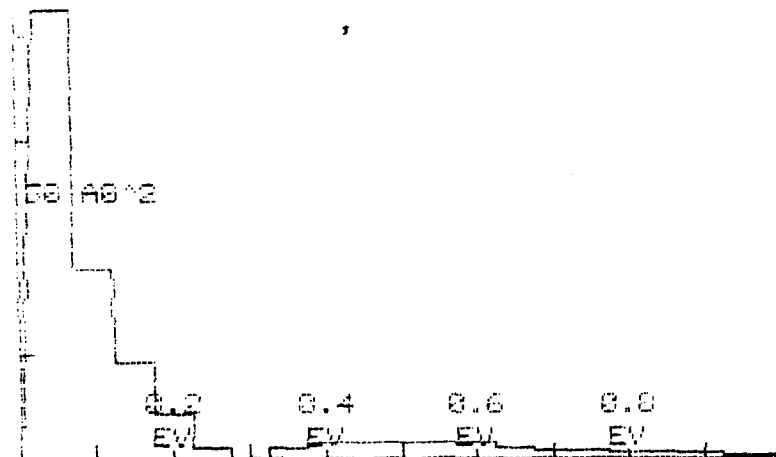
INITIAL V=3



$V=3 \rightarrow \emptyset$

1169 4919

INITIAL V=3



$V=3 \rightarrow 1$

Fig. 9 contd.

1000 AG 12

INITIAL V=3

300 AG 12

$V = 3 \rightarrow 2$

0.2 EV 0.4 EV 0.6 EV 0.8 EV

100 AG 12

INITIAL V=3

30 AG 12

$V = 3 \rightarrow 4$

0.2 EV 0.4 EV 0.6 EV 0.8 EV

Fig. 9 contd.

10 AG 12

INITIAL V=4



$V = 4 \rightarrow 1$

100 AG 12

INITIAL V=4



$V = 4 \rightarrow 2$

Fig. 9 contd.

1000 AG 12

INITIAL V=4



$V = 4 \rightarrow 3$

Fig. 9 contd.

$e^+ p \alpha \rightarrow H + \alpha$

6/21/81

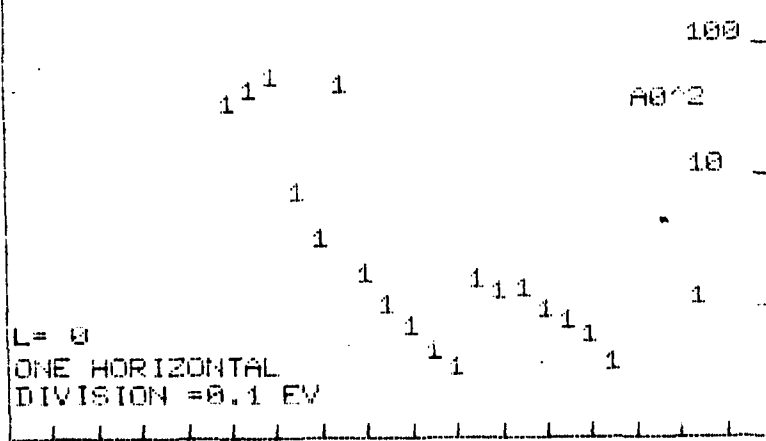
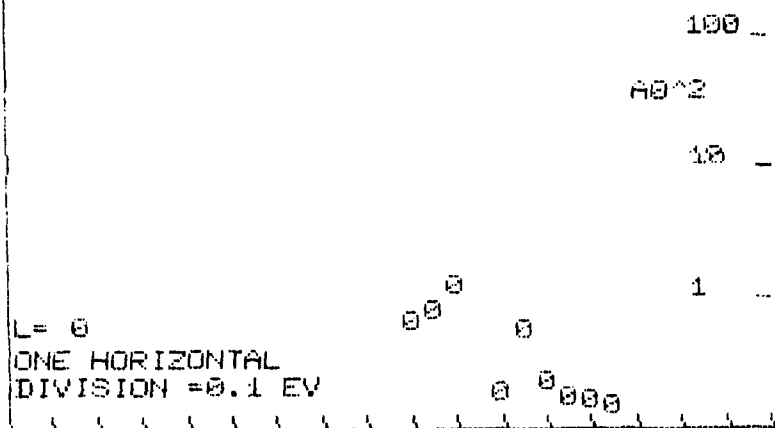


Fig.10a

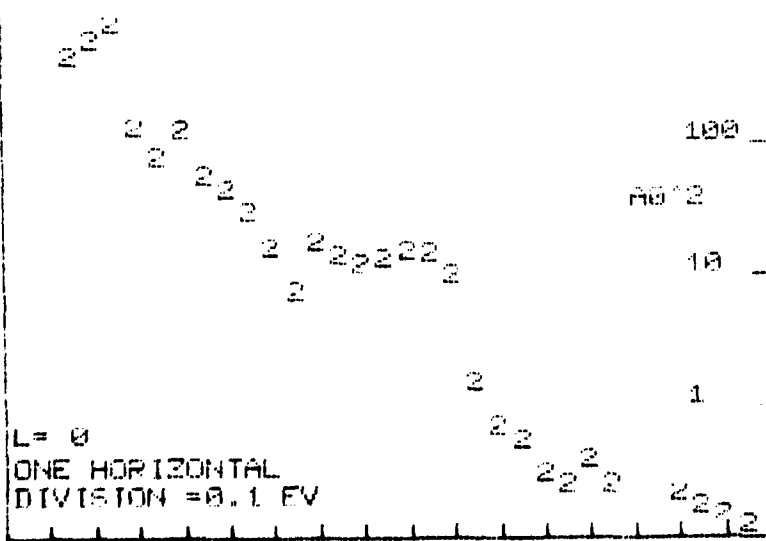


Fig.10a

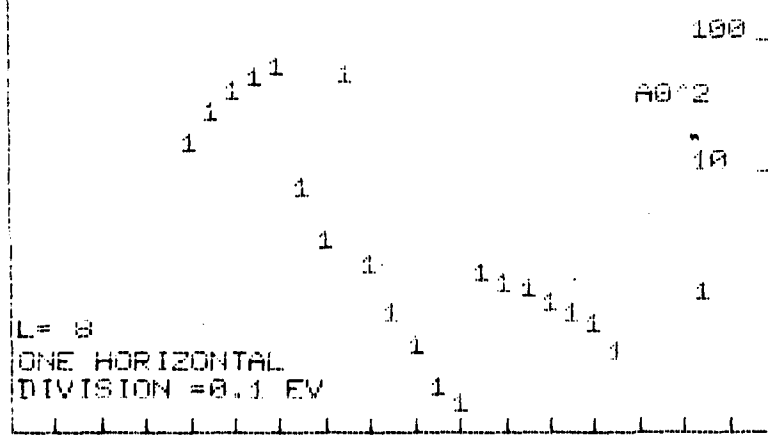
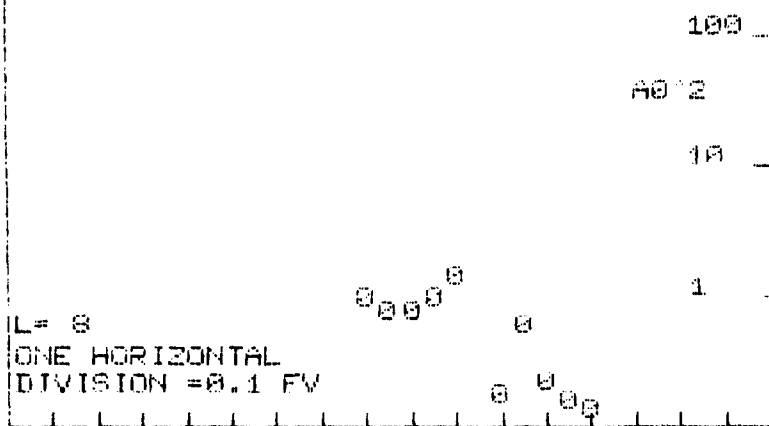


Fig. 10a.

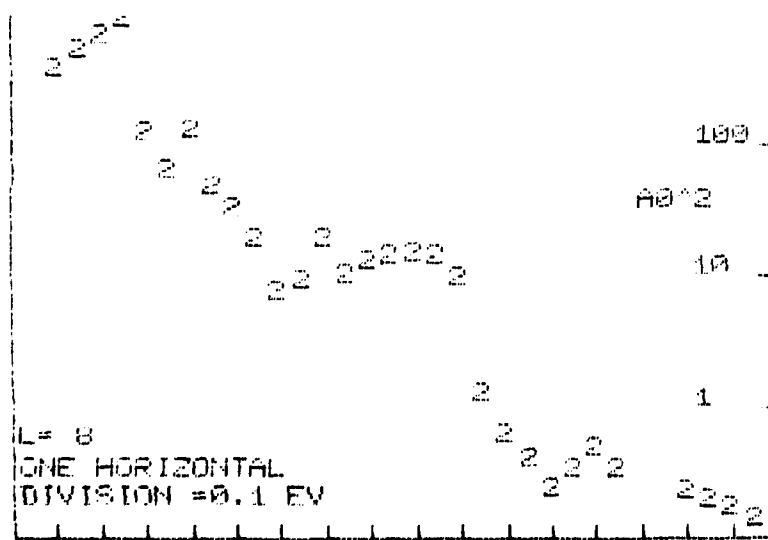


Fig. 10 a cont'd.

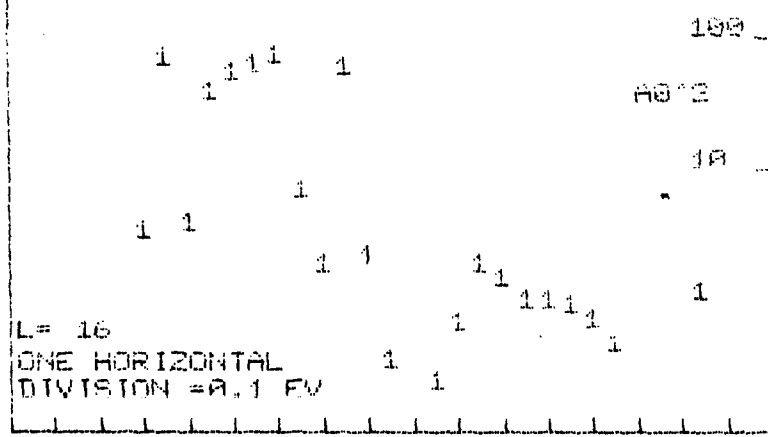
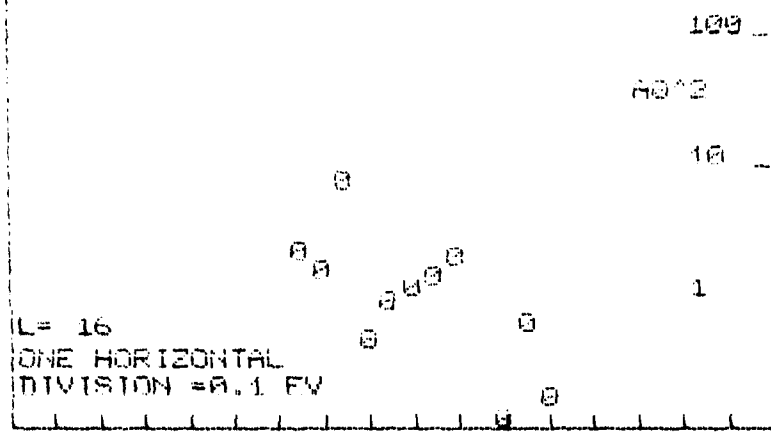


Fig. 102

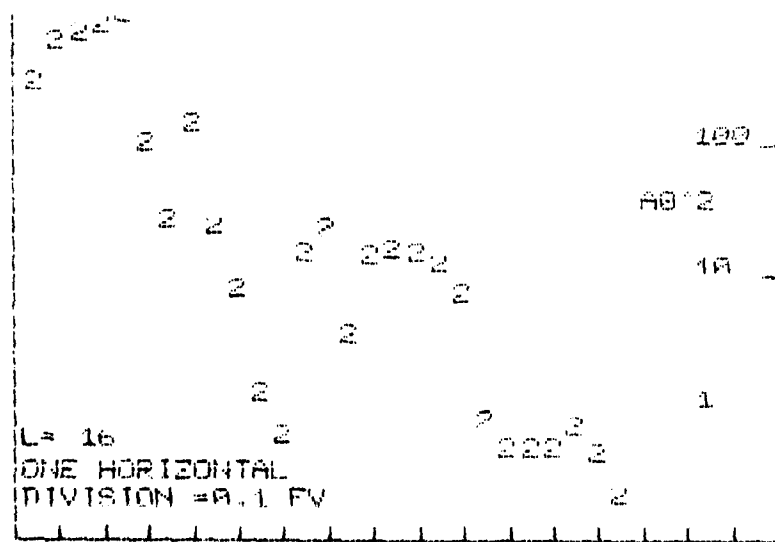


Fig. 10a cont.

YCL  
6/21/81

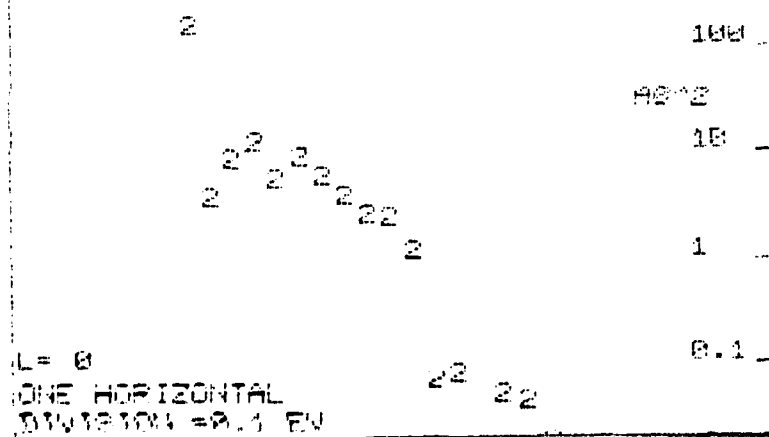
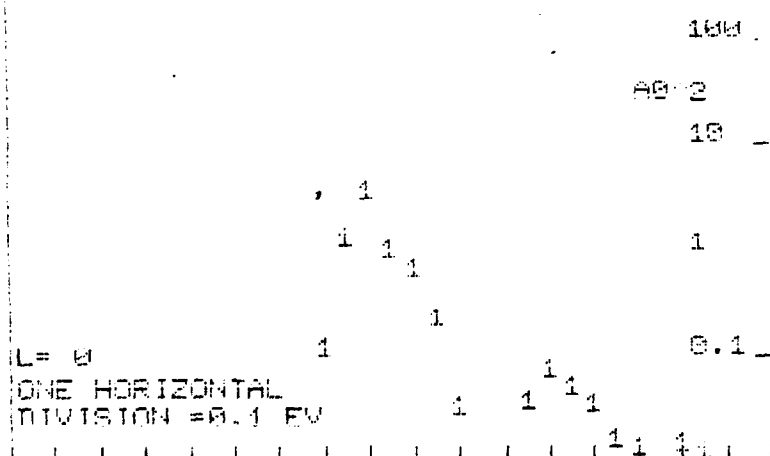
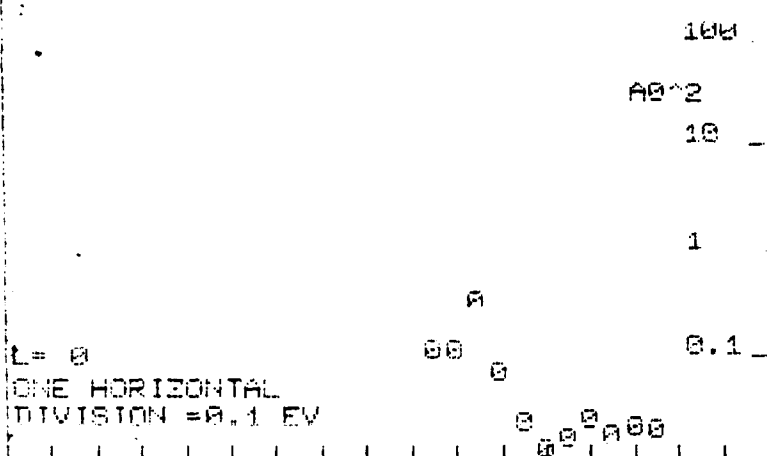
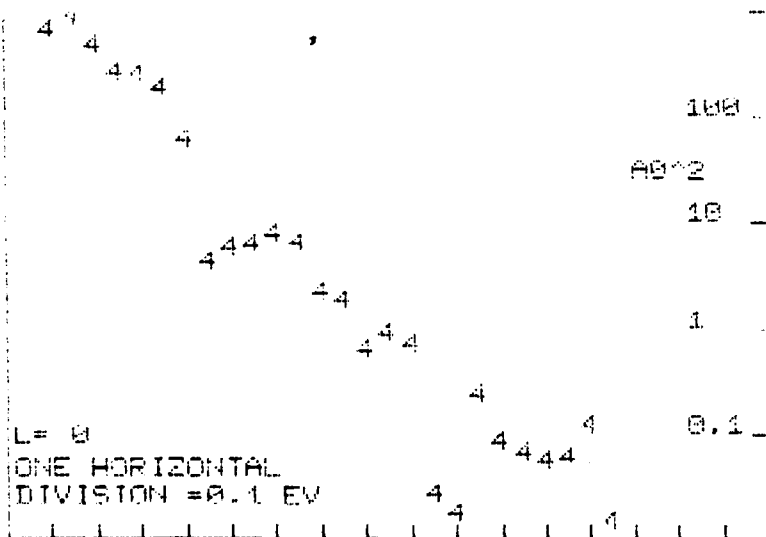
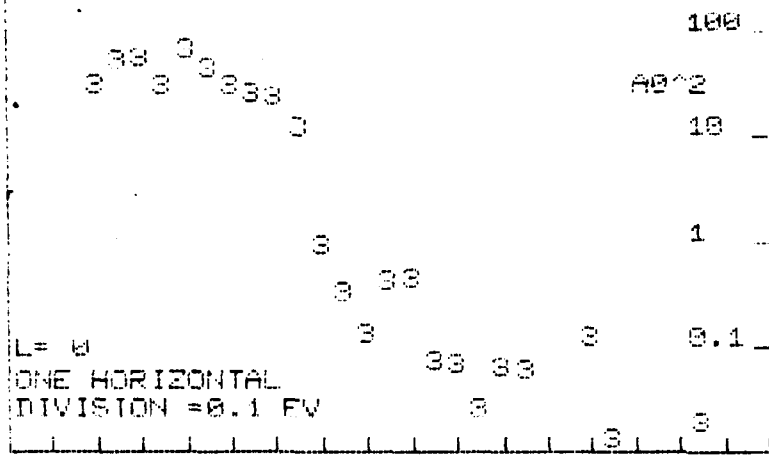


Fig. 10b



$$e + DCl = D + Cl^-$$

$$l_{nuc} = \phi$$

Fig. 10b contd.

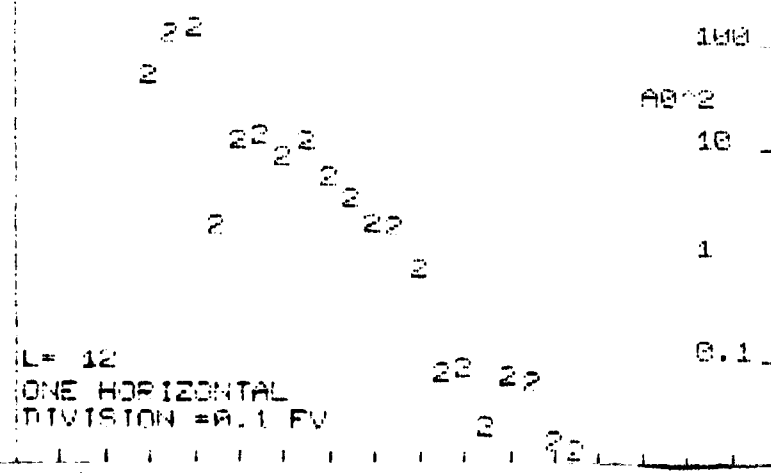
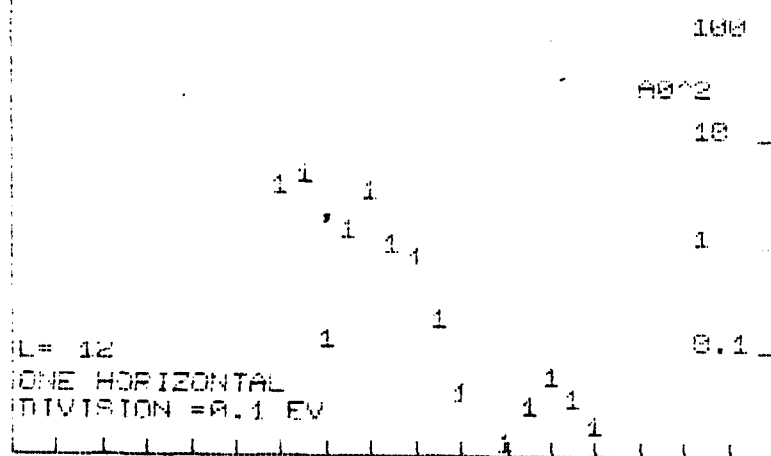
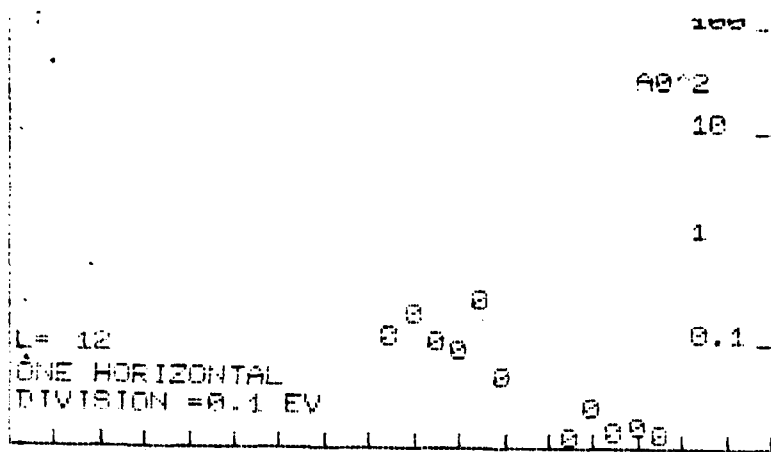
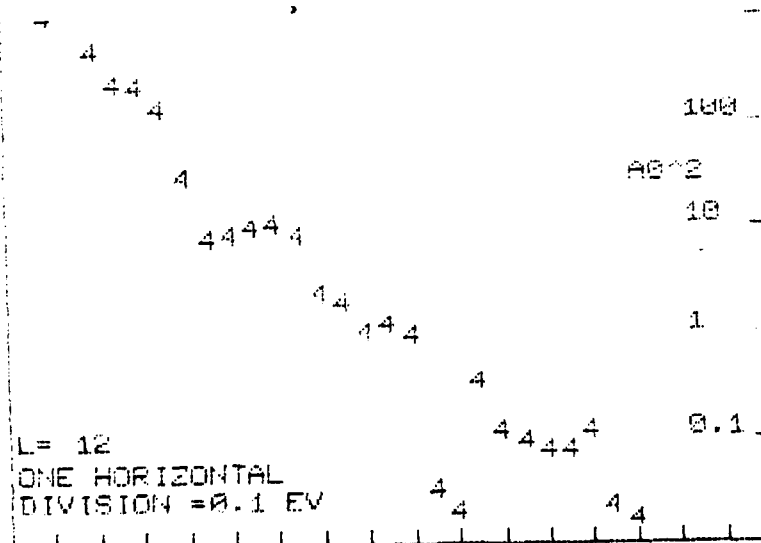
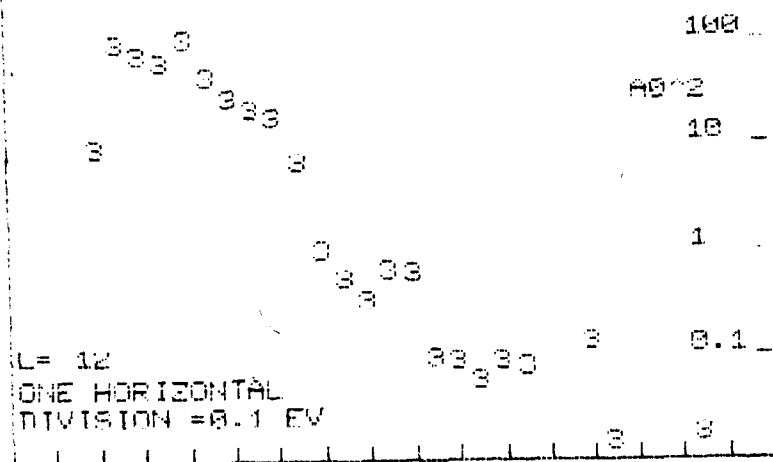


Fig. 10 b contd.



$$l_{\text{max}} = 12$$

Fig 10 b contd.

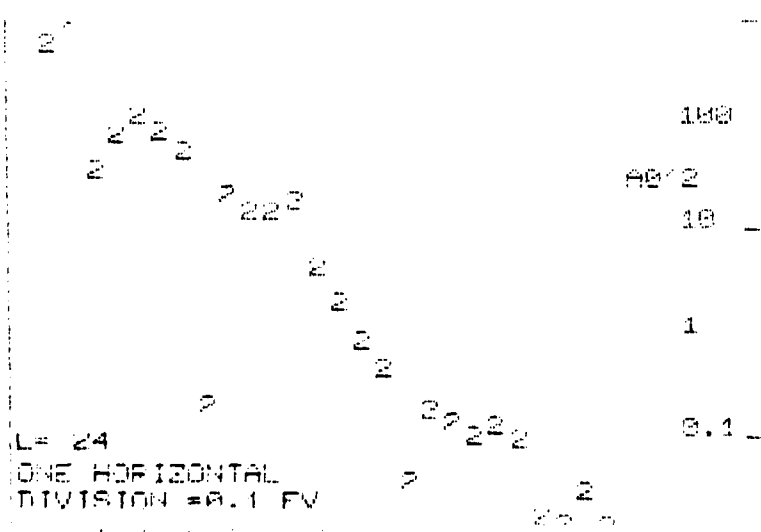
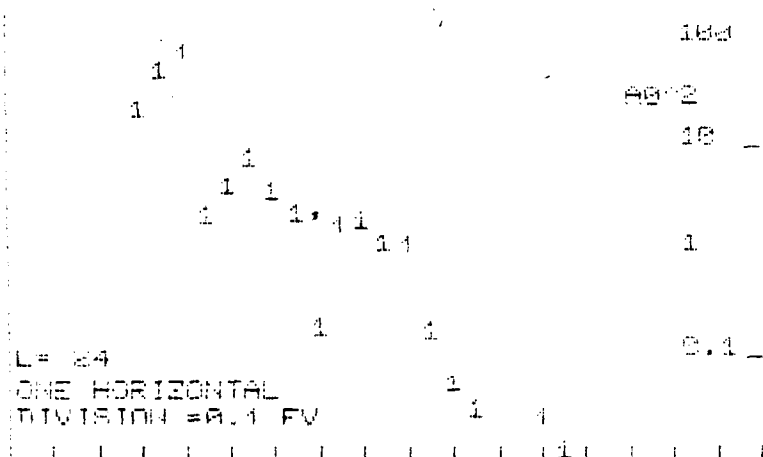
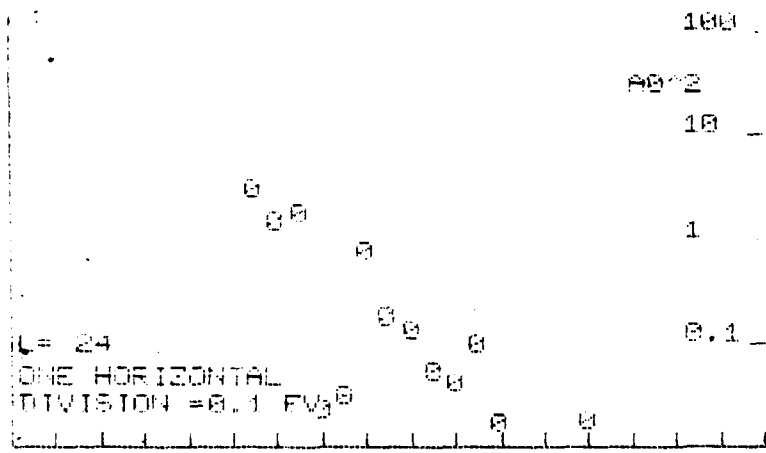
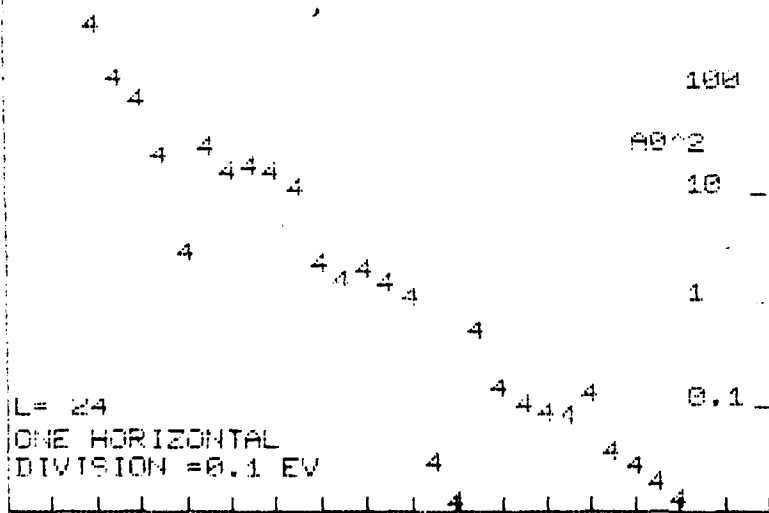
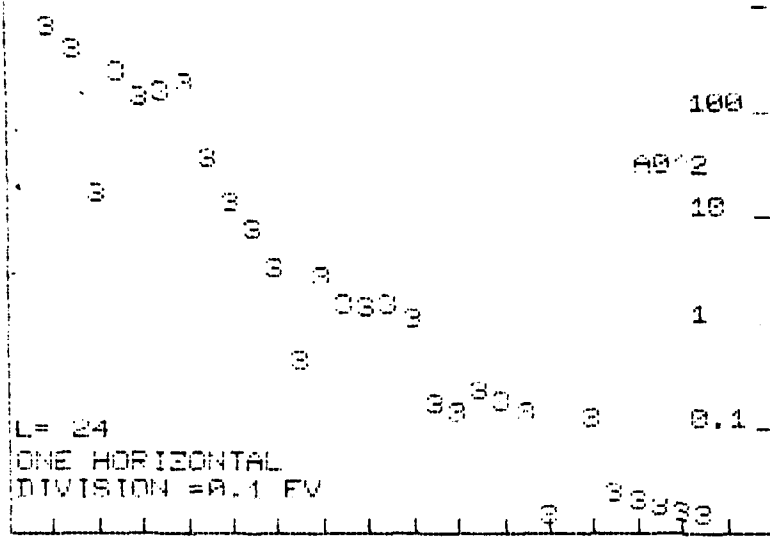


Fig. 10b contd.



$$l_{\text{true}} = 24$$

Fig. 1b contd.

February 1981

REPORTS DISTRIBUTION LIST FOR ONR PHYSICS PROGRAM OFFICE  
UNCLASSIFIED CONTRACTS

Director Defense Advanced Research Projects Agency Attn: Technical Library 1400 Wilson Blvd. Arlington, Virginia 22209	3 copies
Office of Naval Research Physics Program Office (Code 421) 800 North Quincy Street Arlington, Virginia 22217	3 copies
Office of Naval Research Director, Technology (Code 200) 800 North Quincy Street Arlington, Virginia 22217	1 copy
Naval Research Laboratory Department of the Navy Attn: Technical Library Washington, DC 20375	3 copies
Office of the Director of Defense Research and Engineering Information Office Library Branch The Pentagon Washington, DC 20301	3 copies
U. S. Army Research Office Box 12211 Research Triangle Park North Carolina 27709	2 copies
Defense Technical Information Center Cameron Station Alexandria, Virginia 22314	12 copies
Director, National Bureau of Standards Attn: Technical Library Washington, DC 20234	1 copy
Commanding Officer Office of Naval Research Western Regional Office 1030 East Green Street Pasadena, California 91101	3 copies
Commanding Officer Office of Naval Research Eastern/Central Regional Office 666 Summer Street Boston, Massachusetts 02210	3 copies

Commandant of the Marine Corps Scientific Advisor (Code RD-1) Washington, DC 20380	1 copy
Naval Ordnance Station Technical Library Indian Head, Maryland 20640	1 copy
Naval Postgraduate School Technical Library (Code 0212) Monterey, California 93040	1 copy
Naval Missile Center Technical Library (Code 5632.2) Point Mugu, California 93010	1 copy
Naval Ordnance Station Technical Library Louisville, Kentucky 40214	1 copy
Commanding Officer Naval Ocean Research & Development Activity Technical Library NSTL Station, Mississippi 39529	1 copy
Naval Explosive Ordnance Disposal Facility Technical Library Indian Head, Maryland 20640	1 copy
Naval Ocean Systems Center Technical Library San Diego, California 92152	1 copy
Naval Surface Weapons Center Technical Library Silver Spring, Maryland 20910	1 copy
Naval Ship Research and Development Center Central Library (Code L42 and L43) Bethesda, Maryland 20084	1 copy
Naval Avionics Facility Technical Library Indianapolis, Indiana 46218	1 copy

